Forward-Looking GPR Imaging with Near-Optimal 3-D Synthetic Array

Wang, Jianping; Yarovoy, Alexander

Publication date
2019

Document Version
Final published version

Published in
13th European Conference on Antennas and Propagation, EuCAP 2019

Citation (APA)
Wang, J., & Yarovoy, A. (2019). Forward-Looking GPR Imaging with Near-Optimal 3-D Synthetic Array. In *13th European Conference on Antennas and Propagation, EuCAP 2019* (pp. 1-4). Article 8739508 (13th European Conference on Antennas and Propagation, EuCAP 2019). IEEE. https://ieeexplore.ieee.org/document/8739508

Forward-Looking GPR Imaging with Near-Optimal 3-D Synthetic Array

Jianping Wang, Alexander Yarovoy
Microwave Sensing, Signals & Systems (MS3), Delft University of Technology, Delft, The Netherlands
{*J.Wang-4, A.Yarovoy*}*@tudelft.nl*

***Abstract*—In this paper, we propose an Elevation-Radial scanned Synthetic Aperture Radar (E-RadSAR) for forward-looking ground penetrating radar (GPR) imaging. The E-RadSAR exploits the advantages of both RadSAR and Elevation-Circular SAR (E-CSAR) by utilizing the SAR technique in the cross- and down-range directions for signal acquisition. It could be implemented with fewer antennas compared to the RadSAR but provides higher spatial resolutions than that of E-CSAR. These features make it very attractive for space- and/or cost-constrained imaging applications, for instance, the GPR systems used for tunnel boring machines (TBM). However, the E-RadSAR synthesizes a three-dimensional (3-D) array by taking measurements in a volume, which makes the traditional sampling criterion no longer applicable for its sampling strategy design. To tackle 3-D (synthetic) array sampling/design, we formulate it as a sensor selection problem and suggest an efficient selection algorithm, i.e., modified clustered FrameSense (modified CFS). Then it is used for 3-D array sampling design. The imaging performances of the resultant near-optimal 3-D arrays are demonstrated through numerical simulations.**

***Index Terms*—Ground penetrating radar, three-dimensional (3-D) synthetic array, forward-looking imaging, sampling design.**

I. Introduction

Ground penetrating radar (GPR) has been extensively used for subsurface survey, landmine detection, archaeological investigation, hydrogeological studies, to list a few [1]. Recently, a new application scenario for GPR systems is to predict the potential hazard in front of a tunnel boring machine (TBM) during tunnel construction, which is the motivation of the research presented in this paper. For the GPR systems used for TBMs, antennas are installed on their cutter-heads. With the rotation of the cutter-heads, GPR antennas acquire signals at different spatial positions, which naturally leads to a synthetic circular aperture for three-dimensional (3-D) imaging. Specifically, if a linear antenna array is used, a Radial scanned SAR (RadSAR) can be formed [2]. However, due to some space constraints for GPR antenna installation, the number of applicable antennas should be as few as possible.

In literature, circular SAR (CSAR) is the simplest synthetic circular aperture, which can be implemented by using only one antenna [3]. Although it provides three-dimensional imaging capability, the resultant down-range resolution is very low. By further exploiting SAR technique along the down-range direction (i.e., different elevations), Elevation-CSAR (E-CSAR) improves its down-range resolution compared to the CSAR. Although the down-range resolution achieved by E-CSAR is still lower than that obtained by the RadSAR where more antennas are needed, it indicates that exploiting SAR technique along the down-range direction could be a possible way to reduce the number of antennas needed by the imaging system.

As a TBM not only rotates its cutter-head but also moves forward during the tunnel excavation, it provides the opportunity to implement SAR technique in both cross- and down-range directions. Considering this feature, we proposed an Elevation-RadSAR (E-RadSAR) for forward-looking GPR imaging. The E-RadSAR exploits the advantages of both the RadSAR and E-CSAR with attempts to reduce the number of antennas needed but cause little degradation of the spatial resolutions.

To determine the number of antennas needed by the E-RadSAR and the corresponding sampling scheme, it involves a sampling design problem. As the E-RadSAR takes spatial samples in a 3-D volume instead of a plane/surface, it makes the Nyquist sampling criterion and the related sampling design approach no longer applicable. To tackle the 3-D spatial sampling problem, we formulated it as a sensor/observation selection problem and two selection algorithms, i.e., clustered FrameSense (CFS) and clustered maximum projection onto minimum eigenspace (CMPME), have been suggested [4]. Both algorithms aim at selecting a certain amount of samples from a candidate set for sampling design but with different selection optimization criteria. CMPME sequentially chooses the samples whose observation vectors brings the most complementary information relative to those associated with the selected samples while CFS gradually eliminates from the candidate set the samples that bring the largest "frame potential" (a metric of correlation among observation vectors) to the observation matrix. Although CMPME is an efficient selection algorithm and also provides better selection results, it is slightly computationally heavier than CFS where only inner product operations are involved. By minimizing the frame potential of an observation matrix, CFS can only get the optimal selection when all the candidate observation vectors have equal ℓ_2-norms. However, due to the propagation spreading loss of electromagnetic waves and attenuation effects of soil, the observation vectors of GPR measurements apparently have different ℓ_2-norms; thus, the optimality of the selection results of CFS could be degraded. To take advantage of high efficiency of CFS and improve the selection performance in such cases, we propose a modified CFS selection algorithm by considering the distribution of the ℓ_2-norms of the candidate

observation vectors. Based on the distribution of ℓ_2-norm, the modified CFS eliminates the observation vectors with extreme (i.e., maximum/minimum) ℓ_2-norms at the beginning of the selection. Through this operation, the norms of the remaining observation vectors have a more concentrate distribution and then the optimality of the selection results is improved.

The rest of this paper is organized as follows. In section II, the signal model for linear inversion is briefly reviewed. Then, the modified CFS algorithm is presented in section III. After that, some numerical simulations for GPR imaging are performed to show the imaging performance of the selected samples with the proposed selection algorithms. Finally, some conclusions are drawn in section V.

II. Signal Model

Assuming the Born approximation is applicable to scenarios under investigation, the scattering process of GPR signals can be modeled as a linear system [5]

$$\mathbf{y} = \mathbf{A}\mathbf{x} + \mathbf{n} \tag{1}$$

where $\mathbf{y} \in \mathbb{C}^N$ denotes the vector of the scattered signal measurements, $\mathbf{x} \in \mathbb{C}^n$ is the vector of scattering coefficients of the scene which is divided into n cells, and $\mathbf{n} \in \mathbb{C}^n$ represents the vector of measurement errors and noise. $\mathbf{A} \in \mathbb{C}^{N\times n}$ is the observation matrix constructed as rows by the observation vectors related to each measurement. Each entry of $\mathbf{A}$ describes the propagation process of EM waves from a transmitting antenna to a scatterer and then to a receiving antenna through Green's functions.

Equation (1) gives a general model for linear inversion of GPR data. According to (1), N measurements are needed to fully retrieve the scattering properties of scatterers, which could be determined by using sampling theorem based on the resolution requirement and is usually a very large number. However, due to some constraints (e.g., cost, acquisition time, system complexity), it is impractical or impossible to get all N measurements. For instance, GPR antenna systems have a very tight constraint on the number of applicable antennas, which makes that only a certain number of measurements (i.e., fewer than N) can be acquired. Moreover, for E-RadSAR, how to properly take these spatial samples for 3-D high-quality imaging is also a big challenge. To tackle these problems, we convert the sampling problem as a sensor selection problem [4], [5].

Assume only a relatively smaller number of measurements (say, L) can be acquired and the N measurements are the candidate samples. Then taking L measurements for the practical system becomes selecting L samples from the N candidates. Denote the L selected samples as $\mathcal{L} = \{s_1, s_2, \cdots, s_L\}$, the N candidate samples as $\mathcal{N} = \{1, 2, \cdots, N\}$ and $\mathcal{L} \subset \mathcal{N}$. Extracting the equations related to the selected measurements from (1) and putting them together, we get

$$\mathbf{y}_\mathcal{L} = \mathbf{A}_\mathcal{L}\mathbf{x} + \mathbf{n}_\mathcal{L} \tag{2}$$

where $\mathbf{y}_\mathcal{L} \in \mathbb{C}^L$ is a vector of L selected samples and $\mathbf{A}_\mathcal{L}\mathbb{C}^{L\times n}$ is an observation matrix formed by their associated observation vectors. $\mathbf{n}_\mathcal{L} \in \mathbb{C}^L$ is assumed to be a zero-mean circular Gaussian distribution with variance of σ^2, and denotes noise and the measurement errors. Note that the number of selected samples is larger than n, i.e., $L > n$, although it is smaller than N.

Based on the measurements in (2), a minimum variance unbiased estimation of $\mathbf{x}$ obtained via least squares is given by

$$\hat{\mathbf{x}} = \mathbf{A}_\mathcal{L}^\dagger \mathbf{y}_\mathcal{L} \tag{3}$$

where $\mathbf{A}_\mathcal{L}^\dagger = (\mathbf{A}_\mathcal{L}^H \mathbf{A}_\mathcal{L})^{-1}\mathbf{A}_\mathcal{L}^H$ denotes the pseudo-inverse of $\mathbf{A}_\mathcal{L}$. So one can see that the estimation performance of $\hat{\mathbf{x}}$ is determined by the observation matrix, which is typically evaluated through some metrics, such as mean square error (MSE), worst case error variance (WCEV) and condition number.

As each antenna of the E-RadSAR system takes a number of spatial samples, it means selecting one antennas results in choosing a group of observation matrix. So it leads to a vector measurement selection problem [6].

III. Modified Clustered FrameSense

In principle, the vector measurement selection problem related to the sampling design of E-RadSAR can be tackled with many selection algorithms, for instance, convex relaxed optimization, Clustered sequential backward selection (CSBS), CMPME and CFS. Among these algorithms, CFS is the most efficient one. However, it only obtains optimal selection results for observation vectors with equal norms. To improve its selection performance when the observation vectors have nonuniform norms, we suggest a screening scheme based on the distribution of the magnitudes of candidate observation vectors at the beginning stage of CFS so as to optimize the selection results, which is termed as modified CFS.

The modified CFS uses the same cost function as the CFS to gradually eliminate the samples, namely, by minimizing the frame potential of the observation matrix. The major difference is that a screening scheme is introduced before starting the iterative selection procedure. Specifically, for a set of candidate observation vectors with nonuniform norms, we first investigate their norm distribution. Based on the histogram of their ℓ_2-norms, those with the extremely small and big norms are eliminated first. This operation, to some extent, makes the remaining candidates with a homogenized norms, thus alleviating the influence of magnitudes of the observation vectors in the selection results. After that, the same iterative selection operations as the traditional CFS are performed [5]. For the sake of conciseness, we omit the details here.

IV. Numerical Simulations

In this section, a numerical simulation is carried out to optimize a spatial sampling scheme of UWB E-RadSAR for GPR imaging.

GPR synthetic data were generated with the gprMax software by using the Finite Difference Time domain solver

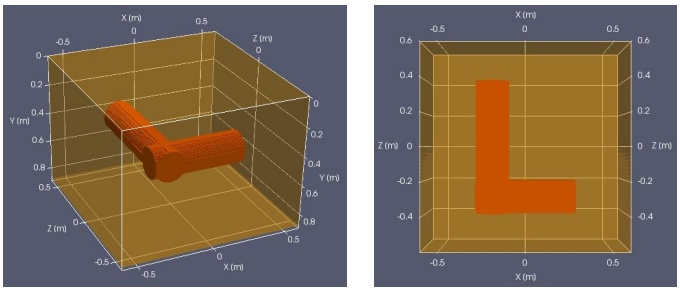

(a) (b)

Fig. 1: The setup for GPR simulation: (a) the 3-D geometrical configuration, and (b) its top view along the positive y-direction.

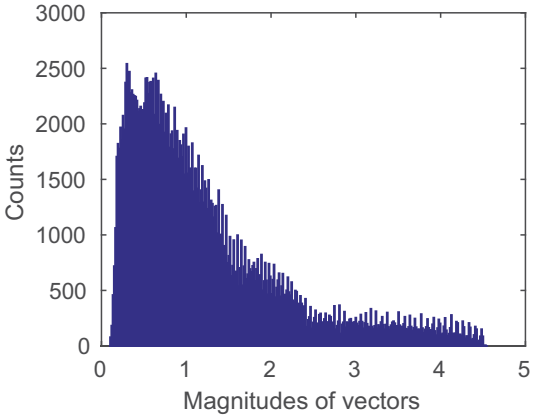

Fig. 2: Histogram of the magnitudes of candidate observation vectors.

(FDTD) [7]. The geometrical setup for the GPR simulation is shown in Fig. 1. In the simulation, an "L"-shaped object formed by two dielectric cylinders of radius 0.1 m was used as targets. The cylinder placed parallel to the z-axis is 0.8m in length while the length of the other one is 0.6m. The "L"-shaped object was buried in a homogeneous background soil. The permittivity of the background soil was 9.0 and the conductivity was 0.01 S/m and the corresponding scattering properties of the cylinders were 5.0 and 0.05 S/m, respectively. The GPR antennas collected the EM signals over a series of concentric circles with the radius ranging from 0.15 to $0.5\,\mathrm{m}$ with steps of $5\,\mathrm{cm}$ on the ground surface. The azimuthal sampling interval is $3°$. Thus, these spatial samples equivalently form a circular aperture array on the ground surface. At each spatial sampling position, the antenna axis was parallel to the radial direction. To emulate the advancement of a TBM during the tunnel excavation, signal measurements were taken at three different elevations with the depths of $0.5\,\mathrm{m}$, $0.4\,\mathrm{m}$ and $0.3\,\mathrm{m}$ relative to the imaging volume of interest below the ground surface. If we take the closest elevation of signal acquisition as the xoz plane, the imaging volume can be defined as a cuboid of $[-0.4, 0.4] \times [0.1, 0.5] \times [-0.5, 0.5]\,\mathrm{m}$. The Ricker

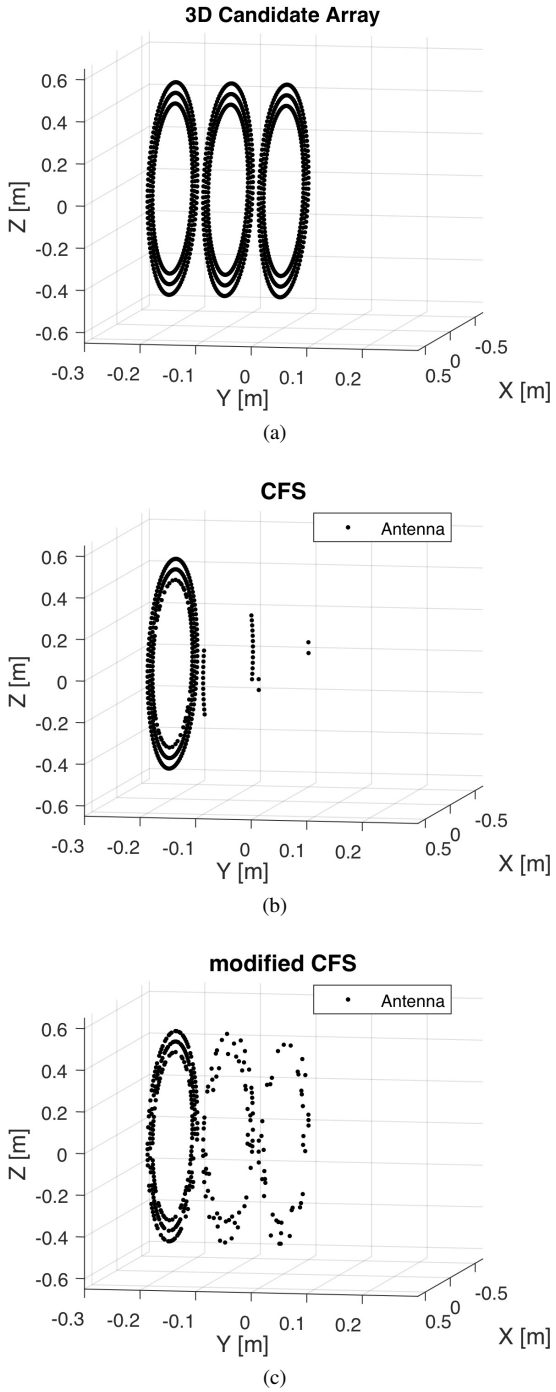

Fig. 3: spatial sampling selection for E-RadSAR system. (a) shows the distribution of candidate samples of three selected antennas, (b) shows the samples selected with CFS, and (c) gives the samples selected with modified CFS.

wavelet of 900 MHz was used as the exciting signal.

Based on the aforementioned sampling scheme, we acquire 2880 (i.e., $8 \times 120 \times 3$) spatial samples in total, which is a set of relatively dense spatial measurements and contains massive redundancy. To fully taking measurements over these spatial samples, eight antennas are needed. However, as indicated in

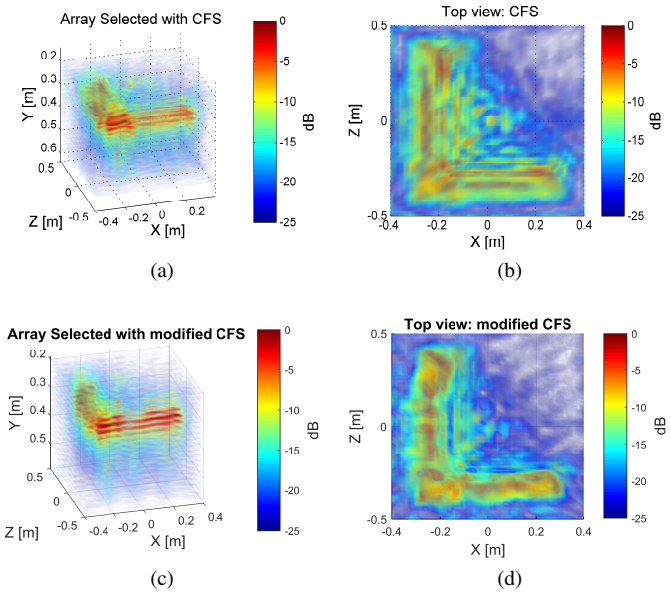

Fig. 4: Image results reconstructed with the spatial samples selected with the two approaches: (a) and (b) CFS; (c) and (d) modified CFS.

section I, this is unacceptable or impractical for some cases with tight constraint on the space occupied by antennas, for instance, GPR systems used for TBMs. So to design the sampling criterion in such cases, we use the aforementioned dense spatial samples as a candidate set and then select a subset of it to get a near-optimal sampling criterion for the E-RadSAR imaging system. As we consider the case with the tight constraint on the number of applicable antennas here, a few of antennas from all the candidates should be firstly selected for the E-RadSAR system. Based on the dimensions of the imaging volume and discretized cells as well as the number of samples acquired by each antennas, it can be determined that at least two antennas are needed for the E-RadSAR system in this example. Then, considering some redundancy, we firstly select three antennas from the eight possible ones by using the CFS. One can see that the outmost three antennas within the circular aperture were selected. Fig. 3(a) shows all the spatial samples that can be acquired by the three selected antennas, which forms a candidate set for further selection of spatial samples for each antenna.

After selecting the applicable antennas, the second step is to determine the sampling scheme for each antenna during the E-RadSAR operation. Fig. 2 shows the histogram of the candidate observation vectors related to all the possible measurement of the three selected antennas. Based on this histogram, we firstly eliminate 5% of the candidates with the extreme norms. Then the traditional CFS and modified CFS are used to design the spatial sampling scheme for the three antennas. The distributions of the spatial samples chosen by CFS and modified CFS are shown in Fig. 3(b) and (c). One can see that the traditional CFS tends to select the samples that are further away from the illuminated volume while the modified CFS selects more samples which are closer to the imaging scene. Due to the different distributions of the spatial samples, images with different focusing performance are reconstructed. For comparison, the reconstructed 3-D images as well as their top-views are shown in Fig. 4. It can be seen that the image with the samples selected by modified CFS has smaller artifacts surrounding the reconstructed "L" shaped object. But a slight distortion is also noticed in Fig 4(d). This is caused by the spatial weighting effects of the antenna radiation patterns. Nevertheless, in terms of the sharpness of the focused image, the modified CFS overperforms the traditional one.

V. Conclusion

In this paper, we investigate the 3-D GPR imaging with the near-optimal 3-D synthetic arrays, i.e., E-RadSAR. To tackle the related sampling design problem, we convert it to a sensor selection problem and a modified CFS is proposed for near-optimal sensor/observation selection. The modified CFS takes advantage of high efficiency of the traditional CFS but also introduces a screening scheme to improve the optimality of the selection results. The effectiveness of this screening scheme has been demonstrated through numerical simulation and the improvement of the imaging performance of the spatial samples selected with modified CFS is observed in contrast to that obtained with CFS.

Acknowledgment

This work was partly supported by the NeTTUN project funded by the European Commission within the FP-7 framework programme under the grant 280712.

References

[1] D. Daniels, *Ground Penetrating Radar, 2nd Edition*. Institution of Engineering and Technology, 2004. [Online]. Available: http://books.google.nl/books?id=iZpEbaJEOy0C

[2] Z. Li, J. Wang, J. Wu, and Q. H. Liu, "A fast radial scanned near-field 3-d sar imaging system and the reconstruction method," *Geoscience and Remote Sensing, IEEE Transactions on*, vol. 53, no. 3, pp. 1355–1363, 2015.

[3] M. Soumekh, *Synthetic Aperture Radar Signal Processing with MATLAB Algorithms*. Wiley, 1999. [Online]. Available: http://books.google.nl/books?id=gVWqQgAACAAJ

[4] J. Wang and A. Yarovoy, "Sampling design of synthetic volume arrays for three-dimensional microwave imaging," *IEEE Transactions on Computational Imaging*, vol. 4, no. 4, pp. 1–13, Dec 2018.

[5] ——, "Near-optimal selection of GPR observations for linear inversion," in *Advanced Ground Penetrating Radar (IWAGPR), 2017 9th International Workshop on*, pp. 1–5.

[6] S. Joshi and S. Boyd, "Sensor selection via convex optimization," *IEEE Transactions on Signal Processing*, vol. 57, no. 2, pp. 451–462, 2009.

[7] C. Warren, A. Giannopoulos, and I. Giannakis, "An advanced gpr modelling framework: The next generation of gprmax," in *2015 8th International Workshop on Advanced Ground Penetrating Radar (IWAGPR)*, July 2015, pp. 1–4.